colloids and interfaces

MDPI

*Article*

# Mannosylerythritol Lipid B Enhances the Skin Permeability of the Water-Soluble Compound Calcein via OH Stretching Vibration Changes

**Yoshihiro Tokudome * and Haruna Tsukiji**

Laboratory of Dermatological Physiology, Department of Pharmaceutical Sciences, Faculty of Pharmacy and Pharmaceutical Sciences, Josai University, 1-1, Keyakidai, Sakado, Saitama 350-0295, Japan

* Correspondence: tokudome@josai.ac.jp

Received: 7 January 2020; Accepted: 19 February 2020; Published: 21 February 2020

**Abstract:** We confirmed that mannosylerythritol lipid B (MEL-B), a biosurfactant, enhances the skin permeability of the model water-soluble compound calcein. MEL-B liposomes were prepared by the thin-layer evaporation technique, and then applied to the skin. Although we attempted to adjust the size by extrusion, we could not control the particle diameter of the liposomes. However, the MEL-B liposome particle diameter remained the same over the 7-day study period. We observed an endothermic peak, with 74.7 °C as the transition temperature by differential scanning calorimetry. We also performed a fusion experiment with a fluorescence resonance energy transfer. A high amount of fusion of intercellular lipid liposomes and MEL-B liposomes occurred in a short period of time. After applying the MEL-B liposomes containing calcein to the skin, we measured the degree of calcein permeation and the amount of calcein within the skin. The resulting values were higher than those of an aqueous solution. The results obtained using a confocal laser scanning microscope suggested that calcein had been delivered deeply into the skin. Using the attenuation of total reflectance Fourier-transform infrared spectrometry, we observed that the OH stretching vibration had shifted to a higher wavenumber; however, this did not affect the CH stretching vibration. The measurement of transepidermal water loss after four days of continuous application of 1% MEL-B to animals revealed no changes. Our results suggest that MEL-B increases the skin permeability of compounds (calcein) that are difficult to deliver transdermally by changing the OH stretching vibration, which shifts to a higher wavenumber.

**Keywords:** mannosylerythritol lipid B; biosurfactant; skin permeation; Fourier-transform infrared spectrometry; hydration of stratum corneum

## 1. Introduction

A surfactant is a material that comprises a mixture of water and oil. Generally, surfactants are used in pharmaceuticals, foods and cosmetics. The body can be severely affected when exposed to surfactants. Surfactants are divided into two types: surfactants derived from natural oils; and naturally derived surfactants. The chief naturally derived surfactants are bile acid and lecithin (phosphatidylcholine) from animals and plants, respectively. Recently, surfactants derived from these natural systems have garnered much attention. Naturally derived surfactants can be amphiphilic when produced by a microbe; these are referred to as biosurfactants (BSs) [1–3]. Existing surfactants and endogenous lipids can possess a variety of bioactivities. As they are biodegradable—a property that is not found in some surfactants—they are expected to be more useful in many fields. BSs are classified based on differences in their structure or their hydrophilic group. BSs with a sugar-

based hydrophilic group have increased productivity, which has prompted the advancement of their use.

Mannosylerythritol lipids, a class of sugar-based BSs, contain a fatty acid as the hydrophobic group linked to mannose, and erythritol as the hydrophilic group linked to the remaining structure [4,5].

Mannosylerythritol lipid B (MEL-B) can easily form large liposomes (lamellar phases) in an aqueous solution. While common surfactants and amphiphilic lipids can easily self-assemble in an aqueous solution to form micelles, only a limited number of substances can form liposomes with a bimolecular membrane structure [6].

It is well-known that phospholipids form liposomes in common surfactants and amphipathic lipids; however, this formation rarely occurs when glycolipids are the sole starting material. MEL-B forms liposomes in wide ranges of concentration and temperature [7]. These properties can therefore be expected to contribute to the stabilization of cosmetic ingredients, and improve the skin permeability of water-soluble compounds. In this study, we prepared MEL-B liposomes, and characterized and evaluated the skin permeability of calcein as a model water-soluble compound.

## 2. Materials and Methods

### *2.1. Materials*

MEL-B in 1,3-butylene glycol was obtained from TOYOBO Co. Ltd (Osaka, Japan). L-$\alpha$-phosphatidylcholine (PC, from an egg) was a gift from Nippon Fine Chemical Co. (Osaka, Japan). Chloroform, methanol and Triton X-100 were purchased from WAKO Pure Chemical Co. Ltd (Osaka, Japan). Ceramide NS and NP were obtained from Matreya (Pleasant Gap, PA, USA). Cholesterol, palmitic acid, cholesterol sulfate and phosphate-buffered saline were purchased from Sigma Aldrich Co. (St. Louis, MO, USA). N-(7-nitro-2-1,3-benzoxadiasol-4-yl)-phosphatidylethanolamine (NBD-PE) and rhodamine-phosphatidylethanolamine (Rho-PE) were obtained from Avanti Polar Lipids Inc. (Alabaster, AL, USA). Calcein sodium was purchased from Tokyo Chemical Industry Co. Ltd (Tokyo, Japan). All other reagents were of analytical grade, and used without further purification.

### *2.2. Animals*

Male HR-1 hairless mice (age, 6 to 7 weeks; body weight, 20–24 g) were obtained from Hoshino Laboratory Animals, Inc. (Bando, Ibaraki, Japan) and maintained in a 12-h light/dark cycle and a temperature-controlled (25 ± 2 °C) environment throughout the study. All mice were allowed to breed for more than one week, and were granted free access to food and water. All animal experiments and maintenance were performed under conditions approved by the animal research committee of Josai University (approval numbers H23024 and H24050).

### *2.3. Preparation of MEL-B Liposomes*

Liposomes were prepared by the thin-layer evaporation technique and freeze-thaw cycling [8,9]. MEL-B was dissolved in chloroform, dried under reduced pressure, and stored in vacuo for at least 1 h. The resulting thin lipid film was hydrated with distilled water. Liposomes were extruded five times through polycarbonate double-membrane filters (pore size: 100, 200 and 400 mm; Nucleopore, Costar, Cambridge, MA, USA). Free lipids in the liposomal suspension were separated by centrifugation (750,000 ×g at 4 °C for 30 min; CS120 EX, Hitachi, Tokyo, Japan). Liposomal pellets were resuspended in distilled water.

### *2.4. Characterization of MEL-B Liposomes*

Particle diameter and zeta potential of MEL-B liposomes

We measured the particle diameter of the MEL-B liposomes by passing the liposomes through a membrane of each pore size. The zeta potential of the surface charge was measured using the

dynamic light scattering method and a Zetasizer Nano ZS (Malvern Instruments Ltd, Worcestershire, UK).

### *2.5. Phase Transition Temperature of MEL-B Liposomes*

The phase transition temperature of MEL-B liposomes was measured using differential scanning calorimetry (DSC, Thermo plus EVO DSC 8230, Rigaku, Tokyo, Japan). The measurement conditions were a temperature ramp rate of 1 °C/min, an atmosphere of air, water as a reference sample and a temperature range of 20–95 °C.

### *2.6. Preparation and Characterization of Stratum Corneum Lipid Liposomes (SCLLs)*

The lipid composition of SCLLs was ceramide (ceramide (NS):ceramide (NP)= 1:1):cholesterol:palmitic acid:cholesterol sulfate = 40:25:25:10 (w/w) [10]. Ceramide, cholesterol and palmitic acid were dissolved in chloroform:methanol (2:1) and cholesterol sulfate in methanol. Liposomes were prepared as described above. Fluorescent-labeled SCLLs were prepared by mixing Rho-PE and NBD-PE with 1 mol% of total lipid.

### *2.7. Fusion Activity of SCLLs*

The measurement of the fusion activity was carried out by the resonance energy transfer method [11,12]. Liposomes were prepared with N-Rho-PE and N-NBD-PE. The final concentration of the two types of fluorescent lipids was 1 mol%. Liposomes were shaken gently in PBS with the SCLLs labeled with fluorescent probes for 24 h at 32 °C; the fluorescence intensity was then measured. Labeled SCLLs were broken down with Triton X-100, and the fluorescence intensity was measured. Liposomal fusion activity was calculated as the percentage of fluorescence intensity of the broken-down SCLLs. The size distribution and zeta potential of liposomes were determined using dynamic light scattering and a submicron particle analyzer. The zeta potential of liposomes was determined using the Zetasizer Nano ZS instrument (Malvern).

### *2.8. Skin Permeation Study in Vitro*

Skin was sampled from the abdominal region to the dorsal regions of male hairless mice (Hos: HR-1, 8–11 weeks old), and fat on the subcutaneous skin layer was removed. Vertical diffusion cells (with an effective permeable area of 1.77 $cm^2$) were attached to the stratum corneum side on the top of the skin. We then added 1 mL each of the 0.5 mM calcein aqueous solution or MEL-B liposomes containing 0.5 mM calcein as the donor solution to the stratum corneum side. The concentrations of MEL-B liposomes were set at 0.5% and 1%. We added 5 mL of distilled water to the receiver solution. The temperature was set at 32 °C, and the experiment was conducted in a closed system.

### *2.9. Measurement of Calcein Concentration in Skin*

After applying the 0.5 mM calcein aqueous solution and MEL-B liposomes containing 0.5 mM of calcein (0.5, 1.0%) for 1, 2 and 4 h, samples remaining on the skin were removed via washing twice with distilled water, after which the skin specimens were collected. The sample application sites were cut off, placed in methanol, and then cut into thin slices using scissors. The sections were then sonicated (20 min) to extract calcein from the skin. The fluorescence intensity (Ex: 488 nm, Em: 515 nm) of the extracted calcein was measured with a spectrophotofluorometer (RF-5300, Shimadzu, Kyoto, Japan).

### *2.10. Preparation of Frozen Sections*

After applying the 0.5 mM calcein aqueous solution and MEL-B liposomes containing 0.5 mM calcein (1.0%) for 1 and 4 h, respectively, samples remaining on the skin were removed by washing twice with distilled water, and the skin specimens were then collected. The sample application sites were cut off, and the skin was embedded in an optimal cutting temperature (OCT) compound. An

adhesive film for frozen sections (Clyofilm, Leica Microsystems, Wetzlar, Germany) was used to prepare 5-μm-thick frozen sections on a Cryostat (Leica CM3050S, Leica Microsystems). The sample was then observed with a confocal laser scanning microscope (OLYMPUS FV1000D IX81, Olympus, Tokyo, Japan).

### *2.11. Measurement of the Skin Permeation of Calcein*

We sampled 0.3 mL of the receiver solution at 24 h after applying 0.5 mM calcein aqueous solution and MEL-B liposomes containing 0.5 mM calcein (0.5, 1%). We mixed 0.1 mL of each of the samples with 0.1 mL of 10 mM EDTA and 0.8 mL of PBS. The skin permeation of calcein was investigated by measuring the calcein fluorescence intensity with a spectrophotofluorometer (Ex: 488 nm, Em: 515 nm).

### *2.12. Collection of Stratum Corneum Sheet for Attenuation of Total Reflectance Fourier Transform Infrared (ATR-FTIR) Measurement*

Using the same methods that were utilized in the skin permeation experiment, we applied MEL-B liposomes (0.5, 1%) to skin collected from hairless male mice (Hos: HR-1, 7–10 weeks old). The MEL-B liposomes remaining on the skin after 1 and 4 h of application were removed with distilled water, and the skin specimens were collected. Heat separation (60 °C, 1 min) was used to collect the stratum corneum. The collected stratum corneum sheets were dried in a desiccator before being humidified in a closed container (temperature: 37 °C, humidity: 75%) containing a saturated saline solution.

### *2.13. ATR-FTIR Spectrophotometry*

The stratum corneum sheets were measured using a Fourier-transform infrared spectrophotometer (FT/IR-5300, Jasco Inc., Easton, US) fitted with a diamond ATR ("Golden Gate", Systems Engineering, Tokyo, Japan). The conditions for the method were an ATR resolution of 0.5 cm-1, a cumulative number of 40, a measurement range of 600–4000 cm-1 and a sample stratum corneum weight of ~3 mg.

### *2.14. Transepidermal Water Loss (TEWL) Measurement*

A 1% synthetic surfactant solution (SDS) and 1% MEL-B liposomes were each applied to the dorsal skin of hairless male mice (Hos: HR-1, 12 weeks old) at 100 μL per day for 4 days, and TEWL was measured over time. TEWL was assessed using a VAPO SCAN AS-VT100 RS (Asahi Techno Lab Ltd, Yokohama, Kanagawa, Japan).

### *2.15. Data Analysis*

All results are shown as mean and standard deviation, and statistical analysis was performed with a Dunnet's multiple comparison test or a Student's t-test using SAS University Edition (SAS Institute Inc., Cary, NC, USA).

## 3. Results

### *3.1. MEL-B Liposome Preparation and Characterization*

We measured the particle diameter of the prepared MEL-B liposomes by passing the liposomes through a polycarbonate membrane with a pore size of 100, 200 or 400 nm. The MEL-B liposomes were prepared on Day 0, and the measurements were obtained on Days 0, 1, 4 and 7. The results are shown in Figure 1a. The particle diameters of the MEL-B liposomes that were passed through the polycarbonate membrane with a pore size of 100, 200 or 400 nm were 160.1, 153.5 and 185.0 nm, respectively. Despite the use of polycarbonate membranes with different pore sizes, no major changes were observed in the measured diameters of the MEL-B liposomes and the particle sizes over the 7-day time course. We then performed a DSC analysis to measure the thermal properties of the MEL-

B liposomes; the results are presented in Figure 1b. The phase transition temperature for the endothermic peak change was 74.7 °C. A summary of these results is presented in Table 1.

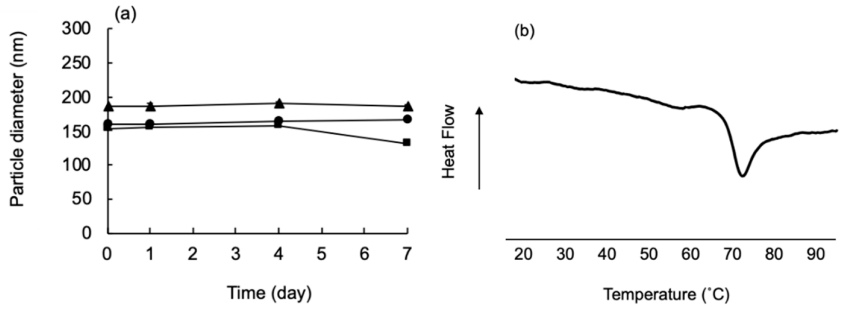


**Figure 1.** Characterization of mannosylerythritol lipid B (MEL-B) liposomes. (a) The change in particle diameter as measured by dynamic light scattering; (b) the thermotropic phase transitions as measured by differential scanning calorimetry (DSC). Symbol: circle, 100 nm; square, 200 nm; and triangle, 400 nm.

**Table 1.** The characteristics of MEL-B liposomes.

| Pore size | Particle diameter (nm) | Phase transition temperature (°C) | Zeta potential (mV) |
|---|---|---|---|
| 100 nm | 160.1 ± 0.12 | 74.7 | –18.9 ± 0.17 |
| 200 nm | 153.5 ± 2.26 | N.T. | N.T. |
| 400 nm | 185.0 ± 2.84 | N.T. | N.T. |

Values are presented as the mean ± S.D. or the mean (only the phase transition temperature) of three experiments. N.T., not tested.

### *3.2. Fusion Rates of Different Liposomes Using Intercellular Lipid Liposomes*

SCLLs labeled with NBD-PE and Rho-PE were used to measure the fusion rates of labeled SCLLs fused with SCLLs, MEL-B liposomes and phospholipid liposomes (dimyristoyl phosphatidyl choline (DMPC) liposomes) over time; the results are shown in Figure 2a. When the fusion rate between intercellular lipid liposomes was set at 100%, the rate in the phospholipid liposomes was lower than the rate between the intercellular lipid liposomes. The MEL-B liposomes exhibited a high fusion rate over a short period of time with the intercellular lipid liposomes. The fusion rate for the MEL-B liposomes and the intercellular lipid liposomes was very high, with a sudden elevation in the fusion rate noted at approximately 30 s (Figure 2b).

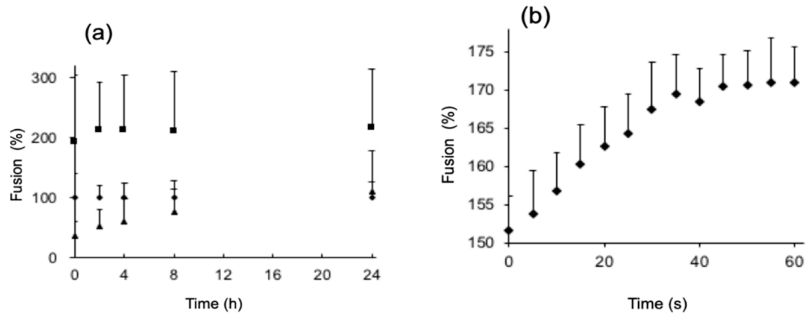


**Figure 2.** Fusion rate of stratum corneum lipid liposomes (SCLLs) with stratum corneum lipid liposomes, DMPC liposomes and MEL-B liposomes. (a) Results up to 24 h; (b) only MEL-B liposomes (60 s). Symbols: closed diamond, SCLLs/SCLLs; closed triangle, DMPC liposomes/SCLLs; closed square, MEL-B liposomes/SCLLs. Values are expressed as the mean ± S.D. of three experiments.

### *3.3. Concentration of Calcein in the Skin after the Skin Permeation Experiment*

Calcein aqueous solution and MEL-B liposomes containing calcein were applied to hairless mouse skin for 1, 2 and 4 h prior to measuring the concentration of calcein in the skin (Figure 3). Compared to the application of the calcein aqueous solution, the application of MEL-B liposomes containing calcein resulted in a greater increase in calcein concentration in the skin. In addition, a greater increase was observed with the application of 1.0% MEL-B liposomes than with the application of 0.5% MEL-B liposomes.

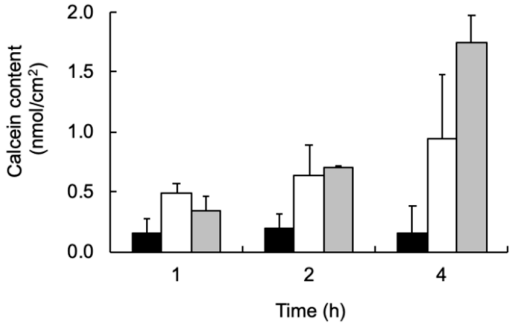


**Figure 3.** Calcein concentration in hairless mouse skin after the application of calcein aqueous solution or MEL-B liposomes containing calcein. Symbols: closed bar, 0.5 mM calcein aqueous solution; open bar, 0.5 mM calcein aqueous solution + 0.5% MEL-B liposomes; gray bar, 0.5 mM calcein aqueous solution + 1.0% MEL-B liposomes. Values are expressed as the mean ± S.D. of three experiments.

### *3.4. Observation of Skin Section Images*

We used a confocal laser microscope to observe skin sections following the skin permeation experiment; these results are shown in Figure 4. When the aqueous calcein solution was applied, the movement of calcein halted in the upper layer of the stratum corneum after 1 and 4 h of application; no marked differences were observed between the two application times. After applying MEL-B liposomes containing calcein for 4 h, however, the calcein in the stratum corneum exhibited a stronger fluorescence, and was observed at deeper sites than the calcein aqueous solution.

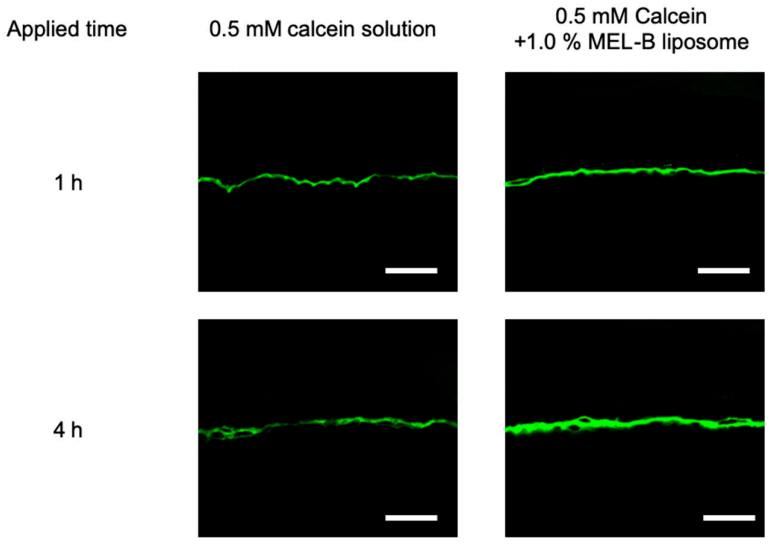


**Figure 4.** Confocal laser scanning microscopy images of a cross-section of the intact skin of a hairless mouse after the application of calcein aqueous solution or MEL-B liposomes containing calcein. The bar indicates 50 μm.

### *3.5. Skin Permeation of Calcein*

We measured the skin permeation of calcein at 24 h after application (Figure 5). Compared to the application of calcein aqueous solution, the application of MEL-B liposomes containing calcein resulted in greater increases in calcein permeation. In addition, the application of 1.0% MEL-B liposomes resulted in a greater increase in permeation than the application of 0.5% MEL-B liposomes.

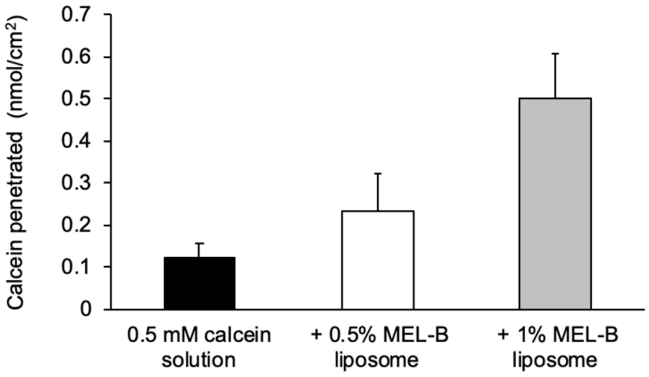


**Figure 5.** Skin permeation of calcein through hairless mouse skin after the application of calcein aqueous solution or MEL-B liposomes containing calcein. Symbols: closed bar, 0.5 mM calcein aqueous solution; open bar, 0.5 mM calcein aqueous solution + 0.5% MEL-B liposomes; gray bar, 0.5 mM calcein aqueous solution + 1.0% MEL-B liposomes. Values are expressed as the mean ± S.D. of three experiments.

### *3.6. Effects of MEL-B Liposomes on the Stratum Corneum*

The stratum corneum to which 0.5% and 0.1% MEL-B liposomes had been applied for 1 and 4 h was examined using ATR-FTIR spectrophotometry, and the results are presented in Table 2. A vehicle (distilled water) was applied to the stratum corneum and denoted the "control". Thus, when compared to normal skin, the application of MEL-B liposomes containing calcein resulted in a shift of the OH stretching vibration to a greater wavenumber.

**Table 2.** OH stretching frequencies following the application of MEL-B liposomes containing calcein to hairless mouse stratum corneum.

| Group | Wavenumber ($cm^{-1}$) | | |
|---|---|---|---|
| | **0 h** | **1 h** | **4 h** |
| Control | 3274.1 ± 1.1 | - | - |
| 0.5% MEL-B | 3274.1 ± 1.1 | 3278.3 ± 1.7 * | 3277.5 ± 3.2 |
| 1.0% MEL-B | 3274.1 ± 1.1 | 3277.2 ± 2.2 | 3279.6 ± 1.8 ** |

Values are expressed as the mean ± S.D. of three experiments. * $p < 0.05$; ** $p < 0.01$ using a Dunnet's test.

### *3.7. Effects of MEL-B Liposomes on Skin Barrier Function*

MEL-B liposomes and SDS aqueous solution were applied to hairless mouse skin, and TEWL was measured over time (Figure 6). TEWL increased significantly with the application of the SDS aqueous solution; however, an increase did not occur with the MEL-B liposomes application (Figure 6).

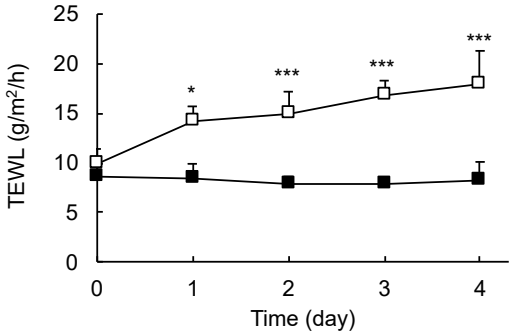


**Figure 6.** Change in TEWL after the application of MEL-B liposomes and SDS solution. Symbols: closed square, 1% MEL-B liposomes; open square, 1% SDS solution. Values are presented as the mean ± S.D. of three experiments. * $p < 0.05$, *** $p < 0.001$ using a Student's t-test.

## 5. Discussion

In this study, we prepared liposomes using MEL-B. In general, a liposome's particle diameter can be adjusted by changing the pore size of the polycarbonate membrane. We attempted to adjust the particle diameters of the MEL-B liposomes; however, this was not achieved despite using membranes with different pore sizes (Figure 1a and Table 1). It appears that after the MEL-B liposomes had passed through the membrane, they may have autonomously adopted a stable form via self-assembly. Moreover, as no changes were observed in the particle diameter over the 7-day measurement period, the MEL-B membrane may have remained stable after formation (Figure 1). MEL-B is a glycolipid and a gemini-type surfactant (i.e., a molecule with two hydrophobic groups and two hydrophilic groups). Some types of gemini-type surfactants with sugar chains in the hydrophilic groups exhibit a smaller association size at increased concentrations. This suggests that as the concentration increases, the hydrogen bonds between hydroxyl groups in the sugar chain region exhibit strong activities, thus forming dense associations [6]. These properties appear to explain the stability and ease of formation that were noted at approximately 160 nm for the 1% MEL-B liposomes that were prepared in this study.

The zeta potential of the MEL-B liposomes indicated that the surface potential was -18.9 mV (Table 1). Generally, applying an electrical charge to liposomes prevents aggregation due to the electrostatic reaction between liposomes, which results in stabilization [13]. As MEL-B liposomes have negative electrical charges, they are unlikely to aggregate, and should remain stable.

The endothermic peak obtained by DSC indicated that the phase transition temperature was 74.7 °C (Figure 1b). This is indicative of the phase transition from the lamellar phase (the liquid crystalline phase) to the mobile phase (isotropic fluid), in which molecules are observed to move randomly. MEL-B is known to form a lamellar phase in a wide range of concentrations and temperatures. Therefore, our results suggest that the lamellar phase had been formed at the concentration present at the time of measurement, and with a temperature of between 20.0 °C and 74.7 °C.

We used the fluorescence resonance energy transfer method to investigate the fusion rates of labeled intercellular lipid liposomes fusing with intercellular lipid liposomes, MEL-B liposomes and phospholipid liposomes (DMPC liposomes). When the fusion rate between intercellular lipid liposomes was set to 100%, we observed a lower fusion rate for the phospholipid liposomes fusing with the intercellular lipid liposomes. In addition, MEL-B liposomes exhibited a high fusion rate over a short period with the intercellular lipid liposomes (Figure 2a). We therefore opted to measure the fusion rate of MEL-B liposomes with intercellular lipid liposomes over an even shorter period of time. In approximately 30 s, a rapid increase of close to 180% occurred in the fusion rate (Figure 2b). As MEL-B liposomes exhibited a high fusion rate with intercellular lipid liposomes, application to skin may also result in a high rate of fusion with intercellular lipids in the stratum corneum. With fluorescence resonance energy transfer (FRET), an increase in the distance between NBD-PE and Rho-PE was found to result in the disappearance of fluorescence polarization, enabling the detection of NBD-PE fluorescence [11,12]. As the same phenomenon not only occurs when liposomes fuse but

when they are destroyed, we measured the particle diameter following the fusion experiment to verify the occurrence of fusion. The mean particle diameter after the fusion of intercellular lipid liposomes and MEL-B liposomes was 253 nm. Unfortunately, when a synthetic surfactant solution (SDS) was applied, the particle diameter could not be measured. Therefore, fusion may have been occurring between the liposomes rather than liposome destruction, as a result of surface action (data not shown). These results indicate that when applied to the skin, MEL-B liposomes will exhibit a high degree of fusion with stratum corneum intercellular lipids. As MEL-B is thought to interact with stratum corneum intercellular lipids, we conducted a skin permeation experiment with skin extracted from mice and containing calcein (an aqueous solution with a relatively large molecular weight) to determine whether MEL-B affects the skin permeability of aqueous compounds. We applied calcein aqueous solution and MEL-B liposomes containing calcein to specimens, and measured the calcein concentration in the skin. Compared to the application of calcein aqueous solution, the application of MEL-B liposomes containing calcein resulted in an increase in the calcein concentration in the skin as the application time increased. The calcein concentration in the skin also tended to increase in a MEL-B liposome concentration-dependent manner (Figure 3). This result suggests that MEL-B liposomes improved the skin permeability of calcein by interacting with intercellular lipids in the stratum corneum. We then observed skin section images following the skin permeation experiment. Compared to the application of calcein aqueous solution, the application of MEL-B liposomes containing calcein resulted in a stronger calcein fluorescence in the stratum corneum, with calcein observed at deeper sites (Figure 4). This result suggests that calcein application, together with MEL-B, facilitates the diffusion and distribution of calcein in the stratum corneum.

Following the skin permeation experiment, we measured the calcein skin permeation volume at 24 h. Compared to the application of calcein aqueous solution, applying the MEL-B liposomes containing calcein resulted in an increase in the transmitted concentration of calcein (Figure 5). These results suggest that applying calcein together with MEL-B liposomes results in an interaction with intercellular lipids to achieve a high degree of distribution within the stratum corneum; this in turn results in an increased volume of calcein being transmitted through the skin.

As we had initially thought, the increase in skin permeability may have been a result of the surface activity of MEL-B destroying the skin barrier. Due to this, we applied MEL-B liposomes to hairless mouse skin and measured TEWL, an index for skin barrier function (Figure 6), but observed no changes in barrier function over the 5-day measurement period. In contrast, TEWL increased in the group in which the SDS aqueous solution was applied. These results show that MEL-B enhances the skin permeability of water-soluble compounds, but it does not exert a surfactant-like action.

Liposomes can internally seal water-soluble and fat-soluble materials in the internal aqueous phase and within the lipid bimolecular membrane, respectively. We therefore sealed calcein within MEL-B liposomes for evaluation. Our results indicated that when calcein is internally sealed, a large particle diameter (over 800 nm) is obtained, which provides poor stability. Therefore, we did not include internally sealed substances in our measurements (data not shown). When we mixed MEL-B liposomes with calcein without sealing it within the MEL-B liposomes, no major changes were observed in the particle diameter. Therefore, it appears that when MEL-B liposomes and calcein are mixed, they take the shape of liposomes. While the details are unclear, OH groups in the aqueous portion of MEL-B create hydrogen bonds with water molecules, which is reported to result in the formation of a stable lamellar structure within the aqueous solution [14]. Therefore, if there are many ions, such as calcein ions, present during liposome formation, this activity may be affected.

To analyze the mechanism underlying skin permeation, we used ATR-FTIR. For the stratum corneum to which MEL-B liposomes had been applied, the peak near 3300 cm-1, representing the stretching vibration, shifted to a higher frequency, compared to the stratum corneum lacking an application of MEL-B liposomes (Table 2) [15]. This result suggests that MEL-B changes the OH vibration of the stratum corneum. Brancaleon has reported on the relationship between OH vibrations and stratum corneum hydration [16]. Furthermore, Olsztyńska-Janus et al. reported an observed shift which indicates the weakening of OH–OH hydrogen bonds between molecules of water [17]. Xi et al. reported a relationship between the transdermal absorption of compounds and

hydrogen bonding [18]. Some researchers have also reported on the relationship between stratum corneum hydration and the skin permeability of water-soluble compounds [19–21]. Therefore, this result suggests that MEL-B increases the skin permeability of compounds by promoting stratum corneum hydration. In addition, Nibu et al., in a study of aqueous mixtures, reported that OH stretching vibrations and the phase state of the membrane are related [22]. This suggests that MEL-B changed the lipid phase in the stratum corneum, resulting in an increase in the calcein penetration into the skin. This suggests that applying MEL-B liposomes may increase the motility of the molecules in the stratum corneum, which in turn may improve the skin permeability of calcein. Results from ATR-FTIR for skin permeability have shown that CH stretching vibrations at 2850 and 2920 cm-1 shift toward a higher frequency, resulting in an increase in liquidity and an improvement in skin permeability [23–27]. Our measurements, however, did not indicate any changes in CH stretching vibrations. Therefore, it appears that a different mechanism improves skin permeability from the one that has previously been reported.

Finally, the difference between MEL-B liposomes and micelles was considered. MEL-B may take the form of micelles or liposomes, depending on the formulation. In general, micelles can encapsulate only oil-soluble compounds. On the other hand, liposomes can capture both oil- and water-soluble compounds; in that regard, liposomes have advantages. From the results of this ATR-FTIR study, it was found that MELB had no significant effect on intercellular lipids of stratum corneum. In general, lipophilic compounds penetrate the skin using lipid layer pathways between the corneocyte in the stratum corneum [28]. Since MEL-B does not significantly affect intercellular lipids, micelles encapsulating lipophilic compounds may not penetrate. On the other hand, the ATR-FTIR investigation suggested that MELB affects the hydrogen bonding or hydration of keratinocytes. This result may be related to the penetration of water-soluble compounds.

## 6. Conclusion

Our results showed that MEL-B liposomes could serve as a useful material for improving the skin permeability of calcein, a highly water-soluble material for which transdermal delivery is difficult. We hypothesized that the skin permeation ability of MEL-B is mediated by its interaction with intercellular lipids in the stratum corneum, rather than its destruction of the stratum corneum's barrier function. Accordingly, we anticipate the application of MEL-B liposomes to water-soluble substances that are difficult to deliver transdermally, as this could contribute to an improvement in their skin permeability.

**Author Contributions:** Conceptualization, Y.T.; methodology, Y.T. and H.T.; formal analysis, Y.T. and H.T.; investigation, Y.T. and H.T.; data curation, Y.T. and H.T.; writing—original draft preparation, Y.T. and H.T.; writing—review and editing, Y.T. and H.T.; visualization, Y.T. and H.T.; supervision, Y.T.; project administration, Y.T. All authors have read and agreed to the published version of the manuscript.

**Funding:** This research received no external funding.
**Conflicts of Interest:** The authors declare no conflicts of interest.

## References

1. Kitamoto, D.; Isoda, H.; Nakahara, T. Functions and potential applications of glycolipid biosurfactants--from energy-saving materials to gene delivery carriers. *J. Biosci. Bioeng.* **2002**, *94*, 187–201.
2. Yu, M.; Liu, Z.; Zeng, G.; Zhong, H.; Liu. Y.; Jiang, Y.; Li, M.; He, X.; He, Y. Characteristics of mannosylerythritol lipids and their environmental potential. *Carbohydr. Res.* **2015**, *407*, 63–72.
3. Ito, S.; Imura, T.; Fukuoka, T.; Morita, T.; Sakai, H.; Abe, M.; Kitamoto, D.; Kinetic studies on the interactions between glycolipid biosurfactant assembled monolayers and various classes of immunoglobulins using surface plasmon resonance. *Colloids Surf. B* **2007**, *58*, 165–171.
4. Morita, T.; Fukuoka, T.; Imura, T.; Kitamoto, D. Production of mannosylerythritol lipids and their application in cosmetics. *Appl. Microbiol. Biotechnol.* **2013**, *97*, 4691–4700.
5. Imura, T.; Hikosaka, Y.; Worakitkanchanakul, W.; Sakai, H.; Abe, M.; Konishi, M.; Minamikawa, H.; Kitamoto, D. Aqueous-Phase Behavior of Natural Glycolipid Biosurfactant Mannosylerythritol Lipid A: Sponge, Cubic, and Lamellar Phases. *Langmuir* **2017**, *23*, 1–5.

6. Worakitkanchanakul, W.; Imura, T.; Fukuoka, T.; Morita, T.; Sakai, H.; Abe, M.; Rujiravanit, R.; Chavadej, S.; Minamikawa, H.; Kitamoto, D. Aqueous-phase behavior and vesicle formation of natural glycolipid biosurfactant, mannosylerythritol lipid-B. *Colloids Surf. B* **2008**, *65*, 106–112.
7. Morita, T.; Fukuoka, T.; Imura, T.; Kitamoto, D. Mannosylerythritol Lipids: Production and Applications. *J. Oleo Sci.* **2015**, *64*, 133–141.
8. Tokudome, Y.; Oku, N.; Doi, K.; Namba, Y.; Okada, S. Antitumor activity of vincristine encapsulated in glucuronide-modified long-circulating liposomes in mice bearing Meth A sarcoma. *Biochim. Biophys. Acta* **1996**, *1279*, 70–74.
9. Hafez, I.M.; Cullis, P.R. Roles of lipid polymorphism in intracellular delivery. *Adv. Drug Deliv. Rev.* **2001**, *47*, 139–148.
10. Wertz, P.W.; Abraham, W.; Landmann, L.; Downing, D.T. Preparation of liposomes from stratum corneum lipids. *J. Invest. Dermatol*. **1986**, *87*, 582–584.
11. Hoekstra, D. Role of lipid phase separations and membrane hydration in phospholipid vesicle fusion. *Biochemistry* **1982**, *21*, 2833–2840.
12. Tokudome, Y.; Saito, Y.; Sato, F.; Kikuchi, M.; Hinokitani, T.; Goto, K. Preparation and characterization of ceramide-based liposomes with high fusion activity and high membrane fluidity. *Colloids Surf. B* **2009**, *73*, 92–96.
13. Oku, N.; Tokudome, Y.; Namba, Y.; Saito, N.; Endo, M.; Hasegawa, Y.; Kawai, M.; Tsukada, H.; Okada, S. Effect of serum protein binding on real-time trafficking of liposomes with different charges analyzed by positron emission tomography. *Biochim. Biophys. Acta* **1996**, *1280*, 149–154.
14. Imura, T.; Yanagishita, H.; Kitamoto, D. Coacervate formation from natural glycolipid: One acetyl group on the headgroup triggers coacervate-to-vesicle transition. *J. Am. Chem. Soc.* **2004**, *126*, 10804–10805.
15. Goh, C.F.; Craig, D.Q.M.; Hadgraft, J.; Lane, M.E. The application of ATR-FTIR spectroscopy and multivariate data analysis to study drug crystallisation in the stratum corneum. *Eur. J. Pharm. Biopharm*. **2017**, *111*, 16–25.
16. Brancaleon, L.; Bamberg, M.P.; Sakamaki, T.; Kollias, N. Attenuated total reflection-fourier transform infrared spectroscopy as a possible method to investigate biophysical parameters of stratum corneum *in vivo*. *J. Invest Dermatol*. **2001**, *116*, 380–386.
17. Olsztyńska-Janus, S.; Pietruszka, A.; Kiełbowicz, Z.,; Czarnecki, M.A. ATR-IR study of skin components: Lipids, proteins and water. Part I: Temperature effect. *Spectrochim. Acta A Mol. Biomol. Spectrosc.* **2018**, *188*, 37–49.
18. Xi, H.; Wang, Z.; Chen, Y.; Li, W.; Sun, L.; Fang, L. The relationship between hydrogen-bonded ion-pair stability and transdermal penetration of lornoxicam with organic amines, *Eur. J. Pharm. Sci.* **2012**, *47*, 325–330.
19. Behl, C.R.; Flynn, G.L.; Kurihara, T.; Harper, U.R.; Smith, W.; Higuchi, W.I.; Ho, N.F.H.; Pierson, C.L. Hydration and percutaneous absorption: I. Influence of hydration on alkanol permeation through hairless mouse skin. *J. Invest. Dermatol.* **1980**, *75*, 346–352.
20. Behl, C.R.; Barrett, M. Hydration and percutaneous absorption II: Influence of hydration on water and alkanol permeation through swiss mouse skin; Comparison with hairless mouse. *J. Pharm. Sci.* **1981**, *70*, 1212–1215.
21. Behl, C.R.; Barrett, X.M.; Flynn, G.L.; Kurihara, Walters, K.A.; Gatmaitan, O.G.; Harper, N., Higuchi, W.I.; Ho, N.F.H.; Pierson, C.L. Hydration and percutaneous 1bsorption III: Influences of stripping and scalding on hydration alteration of the permeability of hairless mouse skin to water and n-alkanols. *J. Pharm. Sci.* **1982**, *71*, 229–234.
22. Nibu, Y.; Inoue, T. Phase behavior of aqueous mixtures of some polyethylene glycol decyl ethers revealed by DSC and FT-IR measurements. *J. Colloid Iinterface Sci.* **1998**, *205*, 305–315.
23. Golden, G.M.; McKie, J.E.; Potts, R.O. Role of stratum corneum lipid fluidity in transdermal drug flux. *J. Pharm. Sci*. **1987**, *76*, 25–28.
24. Higo, N.; Naik, A.; Bommannan, D.B.; Potts, R.O.; Guy, R.H. Validation of reflectance infrared spectroscopy as a quantitative method to measure percutaneous absorption *in vivo*. *Pharm. Res.* **1993**, *10*, 1500–1506.
25. Yokomizo, Y.; Sagitani, H.; Effects of phospholipids on the in vitro percutaneous penetration of prednisolone and analysis of mechanism by using attenuated total reflectance-Fourier transform infrared spectroscopy. *J. Pharm. Sci*. **1996**, *85*, 1220–1226.

26. Cilurzo, F.; Vistoli, G.; Selmin, F.; Gennari, C.G.M.; Musazzi, U.M.; Franzé, S.; Monte, L.M.; Minghetti, P. An insight into the skin penetration enhancement mechanism of N-methylpyrrolidone. *Mol. Pharmaceutics* **2014**, *11*, 1014–1021.
27. Tokudome, Y.; Sugibayashi, K. Mechanism of the synergic effects of calcium chloride and electroporation on the in vitro enhanced skin permeation of drugs. *J. Control. Release* **2004**, *95*, 267–274.
28. Barry, B.W. Mode of action of penetration enhancers in human skin. *J. Control. Release* **1987**, *6*, 85–97.